Arch. Metall. Mater. **70** (2025), 2, 1123-1127

DOI: https://doi.org/10.24425/amm.2025.154454

XIANGYI HAN[1], DONG-GEON LEE[1], SEUNGYOUNG PARK[2], DOO-SEUNG UM[3,4*], CHANG-IL KIM[1*]

REVERSE-PATTERNING PROCESS OF $Ti_3C_2T_x$ MXENE USING AN INKJET PRINTING TECHNIQUE

This study investigated the transformation of conductive MXene films into non-conductive materials using hydrogen peroxide inkjet printing and introduced a novel reverse-patterning technique. Non-conductive patterns can be formed by multiple printing processes of H_2O_2 ink on MXene films to transform $Ti_3C_2T_x$ into TiO_x. X-ray photoelectron spectroscopy analysis confirmed the compositional changes of the MXene films, supporting the fabrication of flexible electronics and custom patterns using the proposed technique. The developed method enhances MXene film integration and can be used to create intricate designs, thereby offering significant potential for use in electronic device manufacturing and materials science.

Keywords: MXene Films; Hydrogen Peroxide Printing; Reverse-patterning; Conductivity Control; Inkjet Printing

1. Introduction

Since the discovery of two-dimensional (2D) graphene in 2004, 2D materials have garnered significant attention because of their unique physical, chemical, and electronic properties, making them ideal candidates for a wide range of applications in optoelectronics, energy storage, sensors, and catalysis [1,2]. Among these materials, transition-metal carbides and carbonitrides, collectively known as MXenes, have emerged as highly versatile systems with remarkable electrical conductivities, tunable surface chemistry, and excellent mechanical properties [3,4]. MXenes are particularly promising for the development of advanced optical and electronic devices owing to their unique characteristics including tunable work functions, excellent charge-transport properties, and plasmonic behavior [5,6]. These features have demonstrated substantial potential for applications in electromagnetic interference shielding, transparent conductive films, and terahertz detectors [7]. However, despite their considerable potential significant challenges remain in realizing their large-scale integration into practical device applications.

A critical aspect of advancing MXene-based technologies is the development of efficient and scalable fabrication methods. Although precise, traditional lithographic techniques are costly, time-consuming, and often incompatible with flexible and wearable devices. In this context, inkjet printing has emerged as an innovative and practical approach for patterning and fabricating 2D material-based electronic and optoelectronic devices [8,9]. Inkjet printing offers several advantages, including low cost, high scalability, and compatibility with a wide variety of substrates ranging from rigid silicon to flexible textiles [10]. This non-contact printing technique can achieve material deposition with high spatial resolution, making it ideal for fabricating intricate electronic circuits and devices under ambient conditions, obviating the need for complex vacuum-based processes.

Moreover, inkjet printing enables the formulation of 2D material-based inks, including MXenes, which can be deposited layer by layer to create heterostructures with properties tailored for specific applications [11,12]. This capability is particularly advantageous for MXenes, as their performance can be significantly enhanced through the precise control of the layer thickness, surface functionality, and interlayer interactions [13,14]. Recent studies have shown promising results for inkjet-printed MXene transistors, sensors, and energy storage devices [15]. However, challenges such as ink formulation optimization, prevention of redispersion during multilayer printing, and clogging of inkjet nozzles must be addressed to fully harness MXenes in commercial-scale applications [16].

To address these limitations, we developed a novel reverse-patterning process, which entails vacuum filtration and wedging transfer methods, to create dense MXene films, followed by

[1] CHUNG-ANG UNIVERSITY, SCHOOL OF ELECTRICAL AND ELECTRONICS ENGINEERING, SEOUL 06974, REPUBLIC OF KOREA
[2] KYONGGI UNIVERSITY, SCHOOL OF ELECTRONIC ENGINEERING, SUWON 16227, REPUBLIC OF KOREA
[3] JEJU NATIONAL UNIVERSITY, DEPARTMENT OF ELECTRONIC ENGINEERING, JEJU 63243, REPUBLIC OF KOREA
[4] JEJU NATIONAL UNIVERSITY, FACULTY OF ENERGY APPLICATION SYSTEM (ELECTRONIC ENGINEERING), JEJU 63243, REPUBLIC OF KOREA

* Corresponding authors: dsum@jejunu.ac.kr; cikim@cau.ac.kr

patterning via the inkjet printing of hydrogen peroxide (H_2O_2). This process eliminates the need to break down MXene into small fragments to prevent the clogging of inkjet nozzles. This, in turn, avoids the reduction of the individual 2D sheet area, which is a common problem in 2D material-based inkjet inks [17]. Additionally, the excellent inkjet jettability of H_2O_2 allows for efficient jetting without requiring further adjustments to the ink formulation. This novel patterning strategy represents a significant advancement in the integration of MXenes into printed electronics and offers new possibilities for their use in next-generation devices.

2. Experimental

$Ti_3C_2T_x$ MXene was prepared by selectively removing Al atoms from Ti_3AlC_2 (Laizhou Kai Kai Ceramic Materials, China) by using a mixture of HF and HCl as the etching agent. The etching solution consisted of 6 mL of hydrochloric acid (35-38%, Sigma Aldrich), 3 mL of hydrofluoric acid (40%, Sigma Aldrich), and 1 mL of deionized (DI) water. This solution was stirred while 1 g of Ti_3AlC_2 powder was gradually introduced at a temperature of 30°C, followed by continuous stirring at 300 rpm for 24 h. The resulting multilayered MXene suspension was rinsed with DI water and centrifuged at 10,000 rpm repeatedly until the pH became neutral (approximately 7). The precipitate was then collected and dispersed in 100 mL of water, to which 20 mL of LiCl solution was added for delamination. The resulting mixture was stirred at 700 rpm for 4 h. The dispersion was further cleaned via centrifugation with DI water until a neutral pH was achieved. Finally, the sediments were redispersed in a small amount of DI water, and the supernatant containing single and few-layer $Ti_3C_2T_x$ MXene flakes was collected after centrifugation at 3,000 rpm [18].

$Ti_3C_2T_x$ MXene films were successfully fabricated via vacuum filtration, where a polydimethylsiloxane (PDMS) thin film with 1 cm diameter pores was placed as a mask on an anodic aluminum oxide (AAO) filter membrane with a pore size of 0.2-μm. A $Ti_3C_2T_x$ MXene solution containing water was prepared at a concentration of 1 mg/mL, and 80 μL of this solution was introduced to obtain circular films with a diameter of 1 cm. After filtration, the films were air-dried at room temperature to ensure proper solvent evaporation. After drying, the $Ti_3C_2T_x$ MXene film that adhered to the filter membrane was detached using the DI water and transferred to a glass substrate that had been treated with ultraviolet ozone (UVO) for 20 min to obtain hydrophilic properties. This wedging transfer method facilitated efficient film handling while minimizing damage. To further enhance the quality and properties of the $Ti_3C_2T_x$ MXene film, an annealing process was conducted on a hot plate at 100°C for 1 h.

The H_2O_2 ink solution used for wound disinfection, purchased from a pharmacy, had a concentration of 3%. Printing was performed using a Dimatix DMP-2850 printer (Fujifilm, Japan) with a Samba G3L printhead (2.4 pL drop volume, 12 nozzles). The piezoelectric head voltage was set to 23 V, with both the ink cartridge and the substrate kept at room temperature. The jetting frequency was 5 kHz and the print height was 0.4 mm. A 10-μm drop spacing was used to avoid ink spreading or excessive dot separation. Only one of the 12 nozzles was used to ensure precise droplet placement.

The surface properties of the MXene films were evaluated using field emission scanning electron microscopy (FE-SEM; Sigma 300, Carl Zeiss). X-ray photoelectron spectroscopy (XPS; NEXSA, Thermo Fisher Scientific) was used to quantify the changes in the concentration of titanium oxide within the MXene films. The electrical properties of the MXene films were analyzed using a digital multimeter (DMM7510; Keithley, USA).

3. Results and discussion

Fig. 1a shows a schematic of the reverse-patterning process for the $Ti_3C_2T_x$ MXene films. High-density $Ti_3C_2T_x$ MXene films were fabricated via vacuum filtration. This approach effectively concentrates MXenes onto anodic aluminum oxide (AAO) membranes, thereby enabling the formation of continuous, dense MXene films with minimal structural defects. To facilitate the transfer of the laminated $Ti_3C_2T_x$ MXene films onto a glass substrate, a wedging transfer method that utilizes the inherent hydrophilicity of $Ti_3C_2T_x$ MXene and the surface tension of water was used [19]. Following this transfer process, annealing was performed on a hot plate to completely remove any remaining moisture from the film surface and interface, thereby improving structural integrity and electrical performance. Subsequently, an inkjet printer was used to precisely spray the H_2O_2 solution according to the predetermined array-printing template. During printing, the $Ti_3C_2T_x$ MXene films reacted with the H_2O_2 solution dropped from the printer, which was oxidized to TiO_x or converted to carbon (C) materials. This series of steps constitutes a complete reverse-patterning process for the conductive MXene electrodes, which can create customized conductive patterns on the substrate. Fig. 1b shows the spider-web pattern printed on MXene films using H_2O_2 ink with a 20-μm line spacing as a function of the number of printing passes. The first image shows the MXene film after being transferred onto a glass substrate using vacuum filtration and a wedging transfer process. The subsequent images, from left to right, represent the inkjet printing results after 5, 10, and 20 printing passes. The spider-web pattern became progressively more pronounced as the number of H_2O_2 ink printing cycles increased. This means that the H_2O_2 ink partially reacted with the MXene film, leading to the formation of materials such as TiO_x and enabling fine patterning of the MXene films. Fig. 1c shows a 2×2 MXene array fabricated using the reverse-patterning process with printed silver electrodes to evaluate the heating characteristics. The inset of Fig. 1c shows a thermal image of a single cell from the MXene heater array, wherein the temperature increased to 45.5°C upon applying 8 V, confirming effective Joule heating and the potential for use in flexible thermal devices. These results show that the reverse-

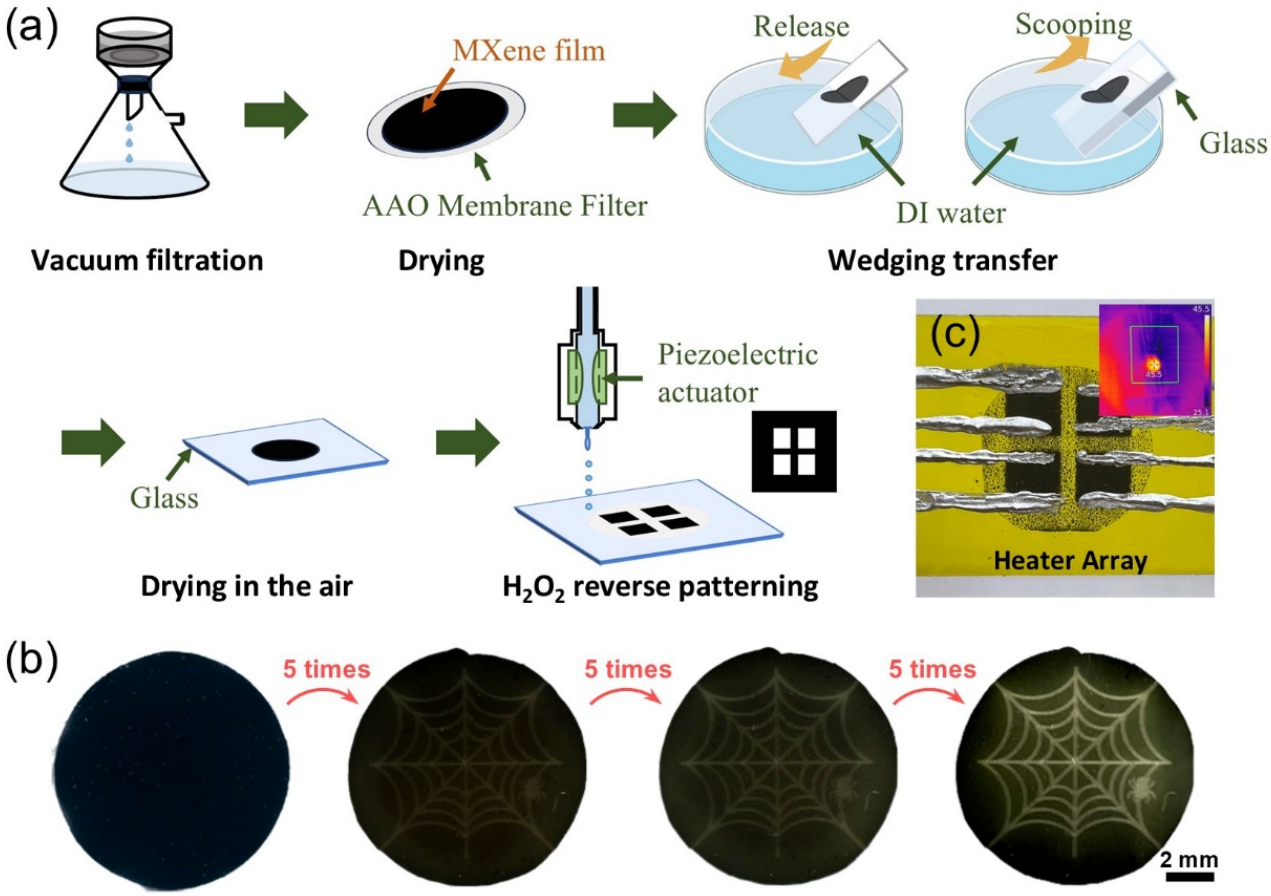

Fig. 1. Manufacturing process of $Ti_3C_2T_x$ MXene films and reverse-patterning via H_2O_2 inkjet printing: (a) detailed schematic of the reverse-patterning process, (b) spider-web patterns formed on the MXene film as a function of the number of H_2O_2 ink printing cycles, and (c) optical and thermographic images of the microheater array device

patterning process has the potential for application in achieving various device configurations.

To investigate whether the conductive MXene film transformed into a non-conductive material through H_2O_2 printing, the central portion of the MXene film between the contact points for resistance measurements was linearly patterned, as shown in Fig. 2a. Changes in resistance were then observed. Fig. 2b shows the clear and distinct line pattern with a 50-µm line width on the MXene film, where 20 passes of H_2O_2 ink were printed. Fig. 2c shows the resistance changes in the MXene film as a function of the line width and number of printing passes, demonstrating that narrower line widths require more printing cycles to fully disrupt conductivity. For a 100-µm line width, the resistance sharply increased after 10 printing cycles, becoming unmeasurable after 15 cycles. At a 50-µm line width, the resistance changed significantly after 15 printing cycles and reached an unmeasurable level beyond 35 cycles. In the case of a 20-µm line width, the resistance started to change rapidly after 55 printing cycles, becoming unmeasurable at 65 cycles. This increase in resistance is attributed to the transformation of the conductive MXene film into a non-conductive material such as TiO_x. This suggests that the reverse-patterning process has potential as a wiring technique for interconnecting devices and systems. Figs. 2d-f show the SEM images of the surface changes in the MXene film caused by the H_2O_2 inkjet printing process. Fig. 2d shows the as-deposited MXene film without the application of H_2O_2 ink. Fig. 2e shows the line created on the MXene film by H_2O_2 printing. Fig. 2f shows a magnified image of the center of the line printed with the H_2O_2 ink after 10 printing passes. Particles that were not visible in Fig. 2d appear in Fig. 2f, suggesting that the MXene sheets transformed into TiO_x particles during the H_2O_2 printing process.

XPS analyses were performed to investigate the compositional changes induced by the reaction between $Ti_3C_2T_x$ MXene and H_2O_2. Fig. 3 presents the XPS spectra of the Ti 2p region in $Ti_3C_2T_x$ MXene. Fig. 3a shows the XPS results for the pristine MXene film, while Fig. 3b depicts the spectra after 10 rounds of H_2O_2 inkjet printing. Deconvolution of the XPS spectra revealed peaks corresponding to TiO_x, Ti-C, Ti^{2+}-C, and Ti^{3+}-C bonds [20]. Notably, the TiO_x peak accounted for 11.76% of the total composition in the pristine MXene film; this increased to 33.2% after 10 rounds of H_2O_2 printing. The reaction between H_2O_2 and $Ti_3C_2T_x$ MXene reduces the conductivity of the materials and induces physical changes such as nanoparticle formation and compositional alterations at the surface [21]. This transformation provides a basis for the application of reverse-patterning techniques in various device fabrication processes wherein conductive MXene can be selectively converted to insulating TiO_x.

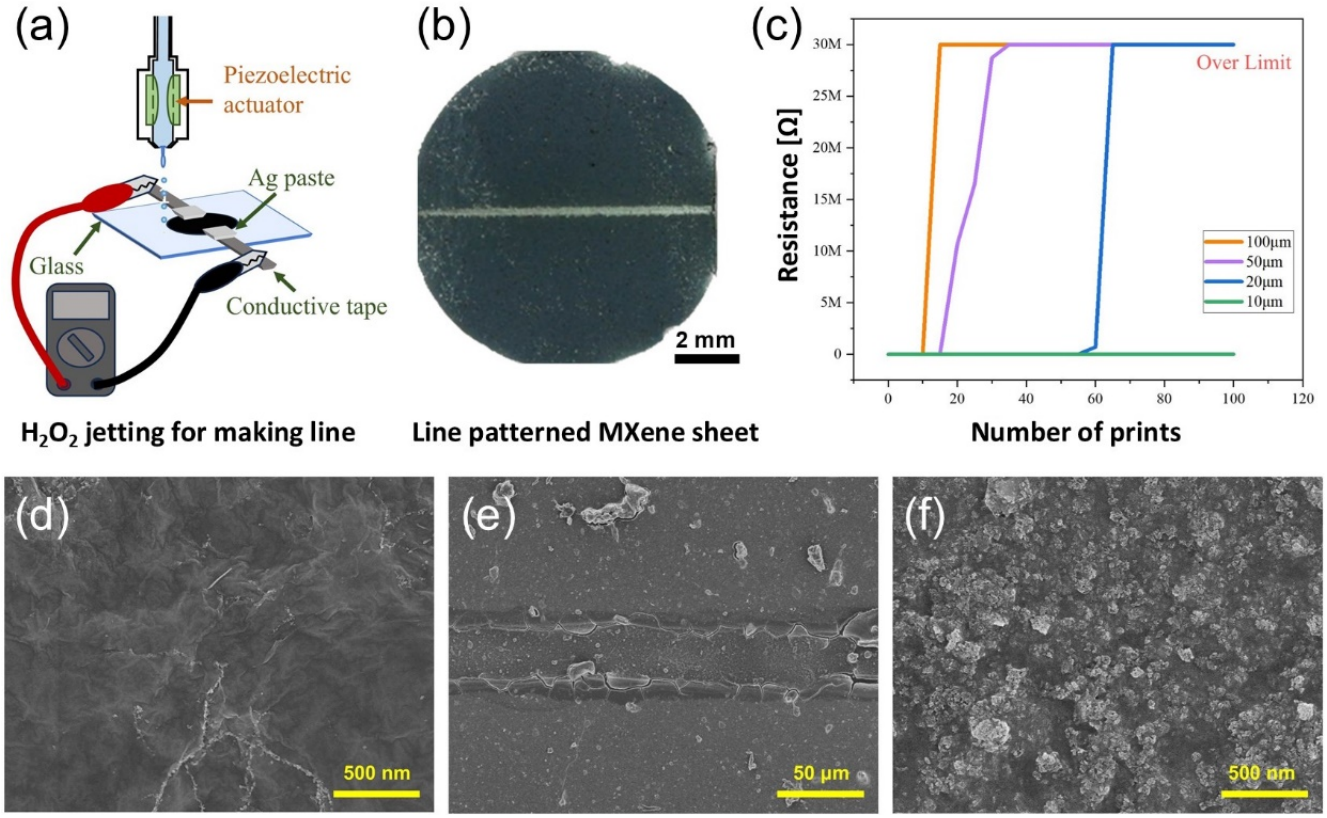

Fig. 2. Resistance changes of $Ti_3C_2T_x$ MXene films through the linear-pattern printing of H_2O_2 ink and the surface characteristics obtained via SEM: (a) the scheme of the experiment, (b) the image after H_2O_2 ink after patterning above the MXene film, (c) Resistance change with repeated H_2O_2 ink patterning, (d) SEM image of the bare film before patterning, (e) SEM image after H_2O_2 ink patterning, and (f) magnified SEM image of the patterned region

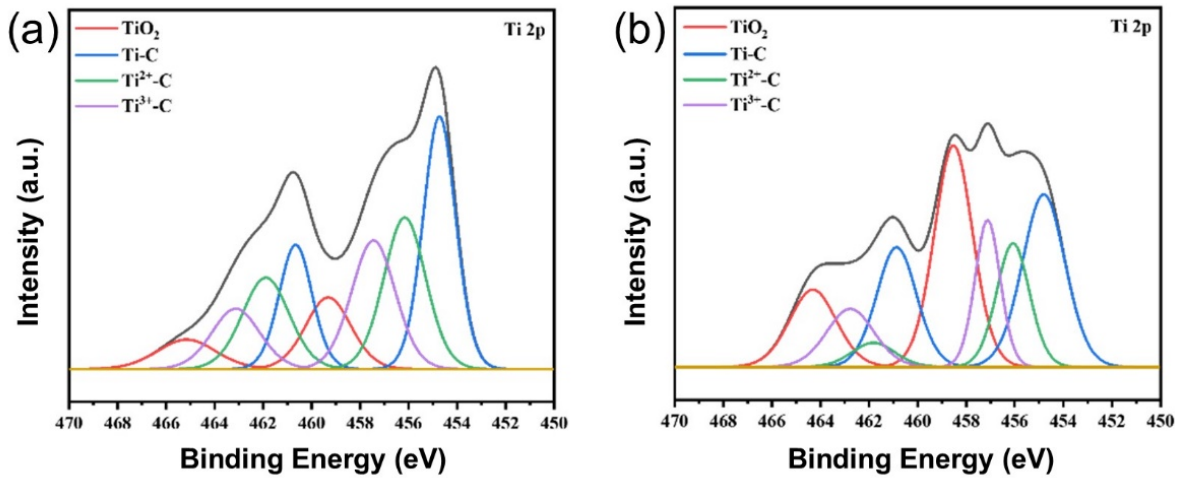

Fig. 3. Surface XPS analysis and deconvolution picks: (a) bare film, and (b) film after undergoing 10 rounds of H_2O_2 printing

4. Conclusions

In this study, we devised a process for the selective formation of nonconductive patterns via inkjet printing using H_2O_2 ink on conductive $Ti_3C_2T_x$ MXene films for fabricating various devices. During this process, $Ti_3C_2T_x$ MXene reacted with H_2O_2 and was converted to TiO_x. Fine patterns could be formed due to the small-sized H_2O_2 ink particles formed by the fine nozzle. We confirmed that the electrical resistance increased as the number of H_2O_2 printing processes increased, and the conductive film was completely converted to a non-conductive material after a certain number of printings. We visually confirmed the surface changes in which TiO_x particles were formed after H_2O_2 inkjet printing through SEM analysis, and XPS analysis showed that the oxidation of $Ti_3C_2T_x$ MXene was accompanied by a chemical transformation to TiO_x. The proposed reverse-patterning process can potentially be applied to the wiring and pattern formation of conductive MXenes in various electronic devices.

Acknowledgments

This work was supported by Korea Institute for Advancement of Technology (KIAT) grant funded by the Korea Government (MOTIE) (P0023718, Inorganic Light-emitting Display Expert Training Program for Display Technology Transition), and "Regional Innovation Strategy (RIS)" through the National Research Foundation of Korea (NRF) funded by the Ministry of Education (MOE) (2023RIS-009).

REFERENCES

[1] D. Ayodhya, A review of recent progress in 2D MXenes: Synthesis, properties, and applications. Diam. Relat. Mat. **132**, 109634 (2023).

[3] Y. Gogotsi, B. Anasori, The Rise of MXenes. ACS Nano. **13**, 8491 (2019).

[5] X. Xu, T. Guo, M. Lanza, H.N. Alshareef, Status and prospects of MXene-based nanoelectronic devices. Matter. **6**, 800 (2023).

[7] M. Iftikhar, F. Shahzad, A. Iqbal, M. Mumtaz, I. Ahmad, T. Hassan, C. M. Koo, Synergistic terahertz shielding effects of electrically conductive MXene and shape-controlled magnetic nickel in polyvinylidene fluoride (PVDF) composites. J. Alloy. Compd. **989**, 174306 (2024).

[8] T. Carey, S. Cacovich, G. Divitini, J. Ren, A. Mansouri, J.M. Kim, C. Wang, C. Ducati, R. Sordan, F. Torrisi, Fully inkjet-printed two-dimensional material field-effect heterojunctions for wearable and textile electronics. Nat. Commun. **8**, 1202 (2017).

[9] X. Sui, S.V. Rangnekar, J. Lee, S.E. Liu, J.R. Downing, L.E. Chaney, X. Yan, H.-J. Jang, H. Pu, X. Shi, S. Zhou, M.C. Hersam, J. Chen, Fully Inkjet-Printed, 2D Materials-Based Field-Effect Transistor for Water Sensing. Adv. Mater. Technol. **8**, 2301288 (2013).

[10] X. Wang, M. Zhang, L. Zhang, J. Xu, X. Xiao, X. Zhang, Inkjet-printed flexible sensors: From function materials, manufacture process, and applications perspective. Mater. Today Commun. **31**, 103263 (2022).

[11] S.P. Sreenilayam, I.U. Ahad, V. Nicolosi, D. Brabazon, MXene materials based printed flexible devices for healthcare, biomedical and energy storage applications. Mater. Today **43**, 99-131 (2021).

[12] M.-J. Jin, D.-S. Um, O. Ogbeide, C.-I. Kim, J.-W. Yoo, J.W.A. Robinson, Crossover from weak anti-localization to weak localization in inkjet-printed $Ti_3C_2T_x$ MXene thin-film. Adv. Nano Res. **13**, 259-267 (2022).

[13] D. McManus, S. Vranic, F. Withers, V. Sanchez-Romaguera, M. Macucci, H. Yang, R. Sorrentino, K. Parvez, S.K. Son, G. Iannaccone, K. Kostarelos, G. Fiori, C. Casiraghi, Water-based and biocompatible 2D crystal inks for all-inkjet-printed heterostructures. Nat. Nanotechnol. **12**, 343-350 (2017).

[14] A. VahidMohammadi, J. Rosen, Y. Gogotsi, The world of two-dimensional carbides and nitrides (MXenes). Science **372**, 3365 (2021).

[15] X. Chen, R. Yang, X. Wu, Printing of MXene-based materials and the applications: a state-of-the-art review. 2D Mater. **9**, 042002 (2022).

[16] O. Song, D. Rhee, J. Kim, Y. Jeon, V. Mazánek, A. Söll, Y.A. Kwon, J.H. Cho, Y.-H. Kim, Z. Sofer, J. Kang, All inkjet-printed electronics based on electrochemically exfoliated two-dimensional metal, semiconductor, and dielectric. npj 2D Mater. Appl. **6**, 64 (2022).

[17] K. Cho, T. Lee, S. Chung, Inkjet printing of two-dimensional van der Waals materials: a new route towards emerging electronic device applications. Nanoscale Horiz. **7**, 1161-1176 (2022).

[18] S. Park, S.H. Ghoi, J.M. Kim, S. Ji, S. Kang, S. Yim, S. Myung, S.K. Kim, S.S. Lee, K.-S. An, Nanoarchitectonics of MXene Derived TiO_2/Graphene with Vertical Alignment for Achieving the Enhanced Supercapacitor Performance. Small **20**, 2305311 (2024).

[19] D.-S. Um, Y. Lee, T. Kim, S. Lim, H. Lee, M. Ha, Z. Khan, S. Kang, M.P. Kim, J.Y. Kim, H. Ko, High-Resolution Filtration Patterning of Silver Nanowire Electrodes for Flexible and Transparent Optoelectronic Devices. ACS Appl. Mater. Interfaces **12**, 32154-32162 (2020).

[20] V. Natu, M. Benchakar, C. Canaff, A. Habrioux, S. Célérier, and M. W. Barsoum, A critical analysis of the X-ray photoelectron spectra of $Ti_3C_2T_z$ MXenes. Matter. **4**, 1224-1251 (2021).

[21] J. Liu, W. Lu, X. Lu, L. Zhang, H. Dong, Y. Li, Versatile $Ti_3C_2T_x$ MXene for free-radical scavenging. Nano Res. **15**, 2558-2566 (2022).